# Articles

## Novel Hyperbranched Polyfluorenes Containing Electron-Transporting Aromatic Triazole as Branch Unit

**Lin-Ren Tsai† and Yun Chen***

*Department of Chemical Engineering, National Cheng Kung University, Tainan, Taiwan*

*Received January 8, 2007; Revised Manuscript Received March 9, 2007*

ABSTRACT: Linear (**P1**) and hyperbranched polyfluorenes (**PF1**−**PF5**) containing hole-transporting [(4-(9-carbazolyl)butoxyphenyl)] side groups and different amounts of branching triphenyl-1,2,4-triazole units (mole fraction: 0−0.22) have been synthesized to investigate hyperbranched structure−optoelectronic property relationship. The hyperbranched polymers have been characterized by NMR, FT-IR, UV−vis, GPC, thermogravimetric analysis, and fluorescence spectroscopy. They show good solubility in common organic solvents such as $CHCl_3$, toluene, and $CH_2Cl_2$ and exhibit excellent thermal stability with decomposition temperatures higher than 446 °C. Their absorption maxima ($\lambda_{max}$) appear at 349−378 nm (both in $CHCl_3$ and in the film state), and furthermore, a linear relationship between $1/\lambda_{max}$ and $1/(1 - n_{triazole})$ has been correlated. The structures of **PF1**−**PF5** effectively suppress detrimental excimer formation (∼550 nm) under thermal annealing. However, in **PF3**−**PF5**, a new PL emission (∼520 nm) appeared after thermal annealing at 200 °C for 1 h, which was attributed to complexes formed from carbazole and triazole chromophores. Both electrochemical results and MNDO semiempirical calculation suggest that oxidation and reduction start from the side carbazole and branching triazole moieties, respectively. Two layer EL devices (ITO/PEDOT/**PF1** or **PF2**/Al) were fabricated and their optoelectronic properties were investigated. The EL spectra of **PF1** and **PF2** are similar to their own PL spectra with the maximum brightness being 161 cd/m$^2$ (at 19.1 V) and 212 cd/m$^2$ (at 19.0 V), respectively.

### Introduction

Recently, electroluminescent (EL) polymers have been extensively investigated owing to their good film-forming properties, easy fabrication via spin-coating, and their tunable luminescence properties, which make them excellent candidates in both single- and multilayer polymer light-emitting diodes (PLEDs).[1] The most extensively studied EL polymers are the linear conjugated ones, such as poly(*p*-phenylenevinylene) (PPV),[1] polyfluorene (PF),[2] and their derivatives.[3] Polyfluorenes (PFs)[2] are promising materials for blue light-emitting diodes because of their high photoluminescence (PL) and electroluminescence (EL) efficiencies.[4] However, there are some drawbacks that hamper their potential applicability, such as the undesired green emission that appears upon thermal annealing or device operation.[5] This low-energy emission band has been attributed to the formation of interchain interaction (excimers or aggregates)[6] in the solid state and/or ketonic defects.[7,8] To minimize interchain interaction, several attempts have been made to use longer and branched side chains or bulky substituents,[9] copolymerization techniques,[10] dendrimer attachment,[11] end-capping of PFs with bulky groups,[12] cross-linking of PFs,[13] and oligomer approach.[10,14]

Recently, hyperbranched polymers have drawn a lot of attention and consideration to diminish formation of interchain interaction due to their highly branched and globular molecular structures.[15] Therefore, light-emitting hyperbranched polymers are of current interest for developing efficient electroluminescent devices and other photonic devices.[16] Moreover, Halim et al. reported that PLEDs made of three-dimensional polymers cause the materials to form good quality amorphous films and to improve thermal stability and emission efficiency.[17] Compared to dendritic polymers,[18] hyperbranched polymers not only are more easy to synthesize but also possess comparable properties. The hyperbranched structure is advantageous over its linear counterpart in high solubility, good processability, and minimization of unfavorable intermolecular interactions and crystallization.[19] In addition, if a hyperbranched polymer has many peripheral chromophores, it will prefer to form a globular structure with generations.[20] By controlling the nature of the end groups, it is possible to endow these hyperbranched architectures with functions such as enhanced adhesion and energy harvesting as well as optoelectronic characteristics. Bo et al. reported the "$AB_2$ + AB" approach to synthesize conjugated hyperbranched polyfluorenes.[21] Another novel "$A_2 + A_2' + B_3$" approach based on Suzuki coupling reaction was also developed for the preparation of hyperbranched polyfluorenes.[22] However, the resulted polymers with high degree of branch were not soluble in common organic solvents.

In this article, in order to avoid the excimer/aggregate formation and to improve the electron affinity and transport ability of PFs, we introduced a 3,4,5-triphenyl-1,2,4-triazole branching unit to prepare hyperbranched polyfluorenes. A novel $A_2 + A_2' + B_3$ approach based on Suzuki condensation coupling was employed for the synthesis of hyperbranched copolyfluorenes **PF1**−**PF5**, in which $A_2$, $A_2'$, and $B_3$ are 9,9-bis[4-(9-

* Corresponding author. E-mail: yunchen@mail.ncku.edu.tw.
† E-mail: n3891123@ccmail.ncku.edu.tw.

10.1021/ma070045l CCC: $37.00 
Published on Web 04/04/2007

carbazolyl)butoxyphenyl] −2,7-dibromofluorene (**M1**), 9,9-dihexylfluorene-2,7-bis(trimethylene boronate) (**M3**) and 3,4,5-tris(4-bromophenyl)-4*H*-1,2,4-triazole (**M2**), respectively. We controlled the reaction time to avoid gelation of the hyperbranched polymers. The resulting hyperbranched triazole-containing polyfluorenes showed stable blue light emission even in the air at elevated temperatures. The influence of branching triazole content on optoelectronic properties of the resulting hyperbranched polymers **PF1**−**PF5** are presented in detail.

## Experimental Section

**Materials.** The synthetic procedures of 2,7-dibromofluorenone (**2**) and 9-(4-bromobutyl)carbazole are described in the literature.[23,24] Phenol (Showa Co.), bromobenzoyl chloride (**3**, Acros Co.), hydrazine monohydrate (Alfa Aesar Co.), phosphorus pentachloride ($PCl_5$, Riedel-Dehaen Co.), *N*-methyl-2-pyrrolidone (NMP, Riedel-Dehaen Co.), chloroform ($CHCl_3$, Tedia Co.), tetrahydrofuran (THF, Tedia Co.), and other solvents were HPLC grade reagents. All reagents and solvents were used without further purification.

**Instrumentations.** All new compounds were identified by $^1$H NMR spectra, FT-IR spectra, and elemental analysis (EA). $^1$H and $^{13}$C NMR spectra were obtained on a Bruker AVANCE-400 NMR spectrometer. The FT-IR spectra were measured as KBr disk using a Fourier transform infrared spectrometer, model Valor III from Jasco. The elemental analysis was carried out on a Heraus CHN-Rapid elemental analyzer. The thermogravimetric analysis (TGA) of the polymers was performed under nitrogen atmosphere at a heating rate of 20 °C/min using a Perkin-Elmer TGA-7 thermal analyzer. Thermal properties of the polymers were measured using a differential scanning calorimeter (DSC), Perkin-Elmer DSC 7, under nitrogen atmosphere at a 20 °C/min heating rate. UV/Visible absorption spectra were measured with a Jasco V-550 spectrophotometer and the photoluminescence (PL) spectra were obtained using a Hitachi F-4500 fluorescence spectrophotometer. The voltammograms of the polymers were measured with a cyclic voltammetric apparatus; model CV-50W from BAS, equipped with a three-electrode cell. The cell was made up of polymer-coated Pt as working electrode, Ag/AgCl electrode as reference electrode, and platinum wire electrode as auxiliary electrode, immersed in acetonitrile containing 0.1 M ($n$-Bu)$_4$NClO$_4$. The energy levels were calculated using the ferrocene (FOC) value of −4.8 eV with respect to vacuum level, which is defined as zero.[25] Polymer light-emitting diodes with a configuration of ITO/ PEDOT:PSS/**PF1** or **PF2**/Al were fabricated, in which the PEDOT: PSS and polymer layers were deposited subsequently by spin-coating method. The film thickness was about 60−100 nm as measured by an atomic force microscope (AFM). The thin layer aluminum was deposited as the cathode by thermal evaporation under a vacuum about $10^{-5}$ Torr. The optoelectronic characteristics of the EL devices were measured by a Keithley power supply (model 2400) and the EL spectra of the device were measured by Ocean Optics usb2000 fluorescence spectrophotometer. All the fabrication and characterization of the devices were under ambient environment.

**Synthesis of Monomers (M1, M2) (Scheme 1). [2,7-Dibromo-9,9-bis(4-hydroxyphenyl)]fluorene (2).** 2,7-Dibromo-9-fluorenone (**1**) (0.50 g, 1.48 mmol), phenol (0.42 g, 4.44 mmol), and Eaton's reagent (3 mL) were put into a 10 mL glass reactor and stirred at 150 °C for 12 h under a nitrogen blanket. The reaction mixture was then poured into water (30 mL) under stirring and extracted with ethyl acetate (60 mL). The combined extracts were dehydrated over $MgSO_4$, dried by evaporation, and then further purified by column chromatography using *n*-hexane/ethyl acetate (v/v = 4/1) as eluent to afford **2** (76%). $^1$H NMR (DMSO-$d_6$): $\delta$ 9.41 (s, 2 H, -OH), 7.89 and 7.87 (d, 2 H, $J$ = 8.1 Hz, Ar−H), 7.57 and 7.55 (d, 2 H, 8.06 Hz, Ar−H), 7.46 (s, 2 H, Ar−H), 6.88 and 6.86 (d, 4 H, $J$ = 8.15 Hz, Ar−H), 6.65 and 6.64 (d, 4 H, $J$ = 8.14 Hz, Ar−H). FT-IR (film, cm$^{-1}$): $\nu$ 3308 (Ar−OH), 3028 (Ar H), 2072, 1502, 1445, 1398, 1322, 1065 (C−Br). Anal. Calcd for $C_{25}H_{16}Br_2O_2$: C, 59.98; H, 3.17; Found: C, 60.02; H, 3.15.

**Scheme 1. Synthesis of Monomers (M1, M2)**

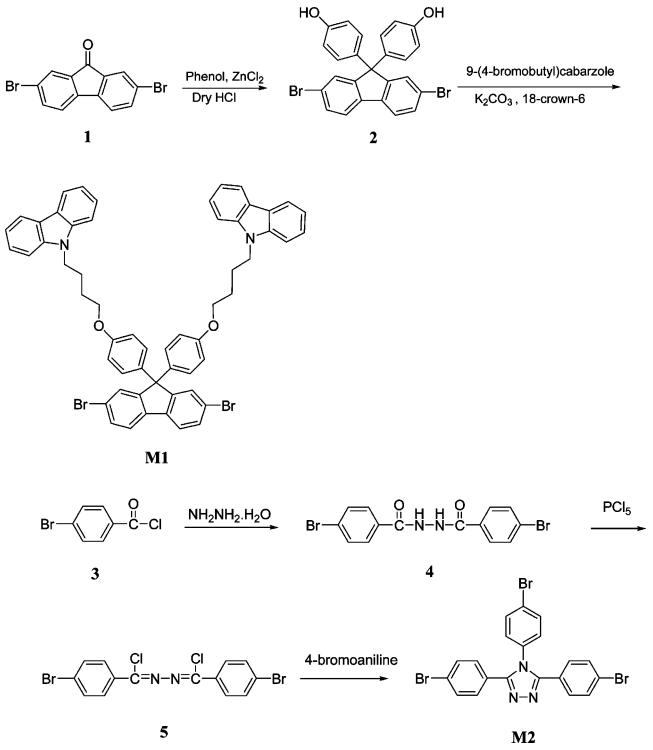


**9,9-Bis[4-(9-carbazolyl)butoxyphenyl]-2,7-dibromofluorene (M1).** 9-(4-Bromobutyl) carbazole was first prepared by reacting 9(*H*)-carbazole (0.33 g, 2 mmol) with excess of 1,4-dibromobutane in an aqueous solution of sodium hydroxide (50%) at 40 °C for 12 h.[17] Reacting of 9-(4-bromobutyl)carbazole (0.47 g, 1.32 mmol) with **2** (0.31 g, 0.6 mmol) in 10 mL cyclohexanone containing excess $K_2CO_3$ (1 g) and a few drops of 18-crown-6 at reflux temperature for 24 h led to **M1** (85%). $^1$H NMR ($CDCl_3$, ppm): $\delta$ 8.09 (d, 4H, $J$ = 7.85 Hz, carbazole rings), 7.57 and 7.55 (d, 2 H, $J$ = 7.95 Hz, Ar−H), 7.46−7.40 (m, 12H, Ar−H), 7.23 (m, 2 H, Ar H), 7.21 (d, 2 H, Ar−H), 7.01 (d, 4 H, Ar−H), 6.72 and 6.71 (d, 4 H, $J$ = 6.8 Hz, Ar−H), 4.40−4.37 (t, 4H, $J$ = 7.05 Hz, N−$CH_2$), 3.90−3.88 (t, 4H, $J$ = 6.05 Hz, $OCH_2$), 2.01 (m, 4H, −$CH_2$−), 1.82 (m, 4H, −$CH_2$−). FT-IR (KBr pellet, cm$^{-1}$): $\nu$ 3045 (Ar H), 2939, 2925, 2855, 1612, 1597, 1502, 1445, 1398, 1322, 1246, 1065 (C−Br). Anal. Calcd for $C_{57}H_{46}Br_2N_2O_2$: C, 72.00; H, 4.88; N, 2.95. Found: C, 71.94; H, 4.78; N, 2.93.

**1,2-Bis(4-bromophenyl)hydrazine (4).** To a two-necked 25 mL flask was charged with 4-bromobenzoyl chloride (**3**: 1.32 g, 6 mmol), hydrazine monohydrate (0.15 g, 3 mmol), and 15 mL NMP. The mixture was stirred at room temperature for 5 h and then precipitated from an excess of distilled water. The appearing products were collected by filtration, washed with ethyl acetate, and dried in vacuum oven to provide **4** (77%). $^1$H NMR (DMSO-$d_6$, ppm): $\delta$ 10.62 (s, 2H, −NH−), 7.85 and 7.83 (d, 4H, $J$ = 8.56, Ar−H), 7.75 and 7.73 (d, 4H, $J$ = 8.52, Ar−H). FT-IR (film, cm$^{-1}$): $\nu$ 3191 (−CONH−), 3016, 2839, 2558, 1684, 1609, 1495, 1468, 1322, 1072 (C−Br), 1011, 931, 840. Anal. Calcd for $C_{14}H_{10}Br_2N_2O_2$: C, 42.24; H, 2.53; N, 7.04. Found: C, 42.28; H, 2.64; N, 7.03.

**1,2-Bis[chloro(4-bromophenyl)methylene]hydrazine (5).** The mixture of **4** (0.84 g, 2.1 mmol) and phosphorus pentachloride (0.96 g, 4.62 mmol) was dissolved in 10 mL toluene and stirred at 120 °C for 3 h under nitrogen atmosphere. After toluene was stripped off under vacuum, the residue was washed twice with distilled water. It was collected by filtration, dried in vacuo, and recrystallized from ethanol and dichloromethane to afford yellow solids of **5** (85%). $^1$H NMR (DMSO-$d_6$, ppm): $\delta$ 8.01 and 8.00 (d, 4H, $J$ = 7.91 Hz, Ar−H), 7.86 and 7.84 (d, 4H, $J$ = 7.74 Hz, Ar−H). FT-IR (film, cm$^{-1}$): $\nu$ 3171, 3080, 2804, 2297, 1910, 1784, 1579 (−N═N−), 1483, 1393, 1222, 1066 (C−Br), 1011, 920, 825.

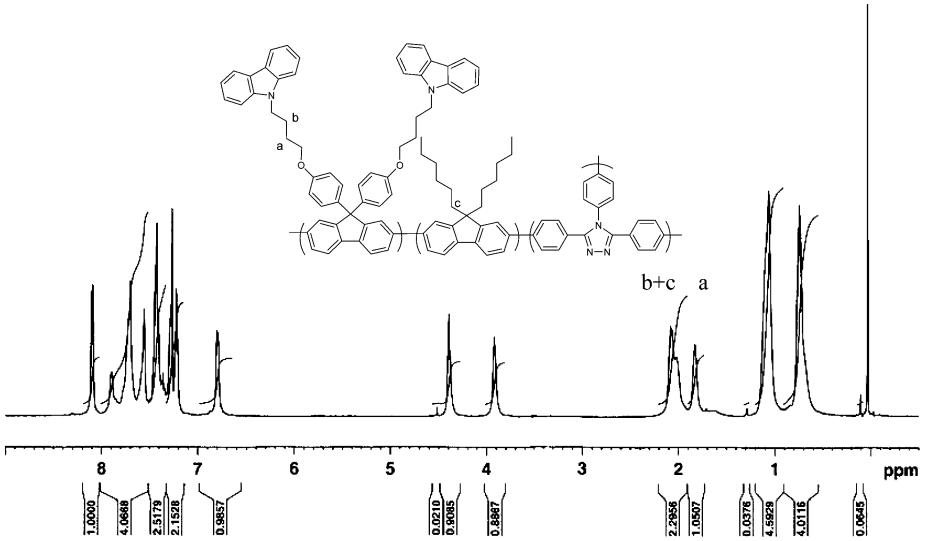


**Figure 1.** $^1$H NMR spectrum of **PF1**.

Anal. Calcd for $C_{14}H_8Br_2Cl_2N_2$: C, 38.66; H, 1.85; N, 6.44. Found: C, 38.67; H, 1.93; N, 6.45.

**3,4,5-Tris(4-bromophenyl)-4*H*-1,2,4-triazole (M2).** The mixture of **5** (0.86 g, 2 mmol), 4-bromoaniline (0.34 g, 2 mmol), and 15 mL of *N*,*N*-dimethylaniline was stirred at 135°C for 12 h under nitrogen atmosphere. After addition 30 mL of 2 N $HCl_{(aq)}$, the mixture was stirred for another 0.5 h. The precipitated solids were collected by filtration, dried and then purified by column chromatography on silica gel using ethyl acetate/*n*-hexane (v/v = 1/2) as eluent. Evaporation of the eluent afforded **M2** (70%). $^1$H NMR ($CDCl_3$, ppm): $\delta$ 7.60 and 7.59 (d, 2H, $J$ = 8.36 Hz, Ar−H), 7.49 and 7.46 (d, 4H, $J$ = 8.44 Hz, Ar−H), 7.27 and 7.25 (d, 2H, $J$ = 8.40 Hz, Ar−H), 7.03 and 7.00 (d, 4 H, $J$ = 8.52 Hz, Ar−H). FT-IR (KBr pellet, cm$^{-1}$): $\nu$ 1058 (C−Br), 2922, 2854, 2360, 1871, 1445, 1414. Anal. Calcd for $C_{20}H_{12}Br_3N_3$: C, 44.98; H, 2.26; N, 7.87. Found: C, 44.59; H, 2.21; N, 7.68.

**Synthesis of Hyperbranched (PF1—PF5) and Linear Polymers (P1).** The general synthetic procedures for the polymers are described as follows: To a solution of predetermined amount of monomers (**M1**, **M2**, and **M3**) in toluene was added with aqueous potassium carbonate (2 M) and ethanol. The mixture was degassed and exchanged with nitrogen three times, and a catalytic amount of tetrakis(triphenylphosphine) palladium [$Pd(PPh_3)_4$] (2.0 mol %) was added in one portion under nitrogen atmosphere. The solution was then stirred at 80 °C under nitrogen. Before gelation, the trace end groups were then capped by refluxing 6 h each with phenylboronic acid and bromobenzene sequentially. After cooling, the resulting polymer was precipitated from methanol twice, collected by filtration, and dried under vacuum.

**PF1: M1** (0.19 g, 0.2 mmol), **M2** (0.02 g, 0.02 mmol), and **M3** (0.13 g, 0.23 mmol), toluene (8 mL), $Pd(PPh_3)_4$ (0.012 g, 0.009 mmol), 2 M aqueous $Na_2CO_3$ solution (4 mL), and ethanol (4 mL) were used. The obtained solid was a light yellow powder (0.18 g, 41%). $^1$H NMR (400 MHz, $CDCl_3$):$\delta$ (ppm) 8.06 (d, $J$ = 7.60 Hz, carbazole rings), 7.78−7.85 (m, Ar−H), 7.63−7.70 (m, Ar−H), 7.55 (m, Ar−H), 7.26−7.48 (m, Ar−H), 6.70 (d, $J$ = 6.30 Hz, Ar−H), 4.30 (t, N−$CH_2$), 3.89 (t, $OCH_2$), 2.03−2.17 (m, −$CH_2$−), 1.74 (m, −$CH_2$−), 1.25 (m, −$CH_2$−), 0.93−0.86 (m, −$CH_2$−), 0.70−0.72 (m, −$CH_3$). FT-IR (KBr pellet, cm$^{-1}$): $\nu$ 3045 (Ar H), 2939, 2922, 2925, 2855, 2360, 1871, 1612, 1597, 1502, 1445, 1414, 1398, 1322, 1246. Anal. Calcd from feed: C, 87.56; H, 6.98; N, 2.68. Found: C, 85.26; H, 7.09; N, 2.58.

**PF2: M1** (0.19 g, 0.2 mmol), **M2** (0.01 g, 0.04 mmol), and **M3** (0.12 g, 0.26 mmol), toluene (8 mL), $Pd(PPh_3)_4$ (0.013 g, 0.01 mmol), 2 M aqueous $Na_2CO_3$ solution (4 mL), and ethanol (4 mL) were used. The obtained solid was a light yellow powder (0.18 g, 41%). $^1$H NMR (400 MHz, $CDCl_3$): $\delta$ (ppm) 8.06 (d, $J$ = 7.58 Hz, carbazole rings), 7.78−7.85 (m, Ar−H), 7.63−7.70 (m, Ar−H), 7.55 (m, Ar−H), 7.26−7.48 (m, Ar−H), 6.70 (d, $J$ = 6.37 Hz, Ar−H), 4.30 (t, N−$CH_2$), 3.89 (t, $OCH_2$), 2.03−2.17 (m, −$CH_2$−), 1.74 (m, −$CH_2$−), 1.25 (m, −$CH_2$−), 0.93−0.86 (m, −$CH_2$−), 0.70−0.72 (m, −$CH_3$). FT-IR (KBr pellet, cm$^{-1}$): $\nu$ 3045 (Ar−H), 2939, 2922, 2925, 2855, 2360, 1871, 1612, 1597, 1502, 1445, 1414, 1398, 1322, 1246. Anal. Calcd from feed: C, 87.51; H, 7.02; N, 2.84. Found: C, 85.61; H, 7.08; N, 2.66.

**PF3: M1** (0.19 g, 0.2 mmol), **M2** (0.035 g, 0.067 mmol) and **M3** (0.15 g, 0.30 mmol), toluene (8 mL), $Pd(PPh_3)_4$ (0.015 g, 0.01 mmol), 2 M aqueous $Na_2CO_3$ solution (4 mL), and ethanol (4 mL) were used. The obtained solid was a light yellow powder (0.21 g,75%). $^1$H NMR (400 MHz, $CDCl_3$): $\delta$ (ppm) 8.06 (d, $J$ = 7.37 Hz, carbazole rings), 7.78−7.85 (m, Ar−H), 7.63−7.70 (m, Ar−H), 7.55 (m, Ar−H), 7.26−7.48 (m, Ar−H), 6.70 (d, $J$ = 6.32 Hz, Ar−H), 4.30 (t, N−$CH_2$), 3.89 (t, $OCH_2$), 2.03−2.17 (m, −$CH_2$−), 1.74 (m, −$CH_2$−), 1.25 (m, −$CH_2$−), 0.93−0.86 (m, −$CH_2$−), 0.70−0.72 (m, −$CH_3$). FT-IR (KBr pellet, cm$^{-1}$): $\nu$ 3045 (Ar−H), 2939, 2922, 2925, 2855, 2360, 1871, 1612, 1597, 1502, 1445, 1414, 1398, 1322, 1246. Anal. Calcd from feed: C, 87.45; H, 7.06; N, 3.03. Found: C, 87.81; H, 7.36; N, 3.12.

**PF4: M1** (0.19 g, 0.2 mmol), **M2** (0.05 g, 0.1 mmol) and **M3** (0.17 g, 0.35 mmol), toluene (8 mL), $Pd(PPh_3)_4$ (0.017 g, 0.013 mmol), 2 M aqueous $Na_2CO_3$ solution (4 mL) and ethanol (4 mL) were reacted. The obtained solid was a light yellow powder (0.16 g, 52%). $^1$H NMR (400 MHz, $CDCl_3$): $\delta$ (ppm) 8.06 (d, $J$ = 7.62 Hz, carbazole rings), 7.78−7.85 (m, Ar−H), 7.63−7.70 (m, Ar−H), 7.55 (m, Ar−H), 7.26−7.48 (m, Ar−H), 6.70 (d, $J$ = 6.60 Hz, Ar−H), 4.30 (t, N−$CH_2$), 3.89 (t, $OCH_2$), 2.03−2.17 (m, −$CH_2$−), 1.74 (m, −$CH_2$−), 1.25 (m, −$CH_2$−), 0.93−0.86 (m, −$CH_2$−), 0.70−0.72 (m, −$CH_3$). FT-IR (KBr pellet, cm$^{-1}$): $\nu$ 3045 (Ar−H), 2939, 2922, 2925, 2855, 2360, 1871, 1612, 1597, 1502, 1445, 1414, 1398, 1322, 1246. Anal. Calcd from feed: C, 87.43; H, 7.30; N, 3.22. Found: C, 86.41; H, 7.52; N, 3.33.

**PF5: M1** (0.19 g, 0.2 mmol), **M2** (0.11 g, 0.2 mmol) and **M3** (0.25 g, 0.5 mmol), toluene (8 mL), $Pd(PPh_3)_4$ (0.024 g, 0.018 mmol), 2 M aqueous $Na_2CO_3$ solution (4 mL) and ethanol (4 mL) were used. The obtained solid was a light yellow powder (0.21 g, 54%). $^1$H NMR (400 MHz, $CDCl_3$): $\delta$ (ppm) 8.06 (d, $J$ = 7.43 Hz, carbazole rings), 7.78−7.85 (m, Ar−H), 7.63−7.70 (m, Ar−H), 7.55 (m, Ar−H), 7.26−7.48 (m, Ar−H), 6.70 (d, $J$ = 6.30 Hz, Ar−H), 4.30 (t, N−$CH_2$), 3.89 (t, $OCH_2$), 2.03−2.17 (m, −$CH_2$−), 1.74 (m, −$CH_2$−), 1.25 (m, −$CH_2$−), 0.93−0.86 (m, −$CH_2$−), 0.70−0.72 (m, −$CH_3$). FT-IR (KBr pellet, cm$^{-1}$): $\nu$ 3045 (Ar H), 2939, 2922, 2925, 2855, 2360, 1871, 1612, 1597, 1502, 1445, 1414, 1398, 1322, 1246. Anal. Calcd from feed: C, 87.33; H, 7.20; N, 3.65. Found: C, 86.06; H, 7.69; N, 3.44.

**P1: M1** (0.19 g, 0.2 mmol), **M3** (0.10 g, 0.2 mmol), toluene (8 mL), $Pd(PPh_3)_4$ (0.011 g, 0.008 mmol), 2 M aqueous $Na_2CO_3$

**Scheme 2. Synthesis of P1 and PF1−PF5**

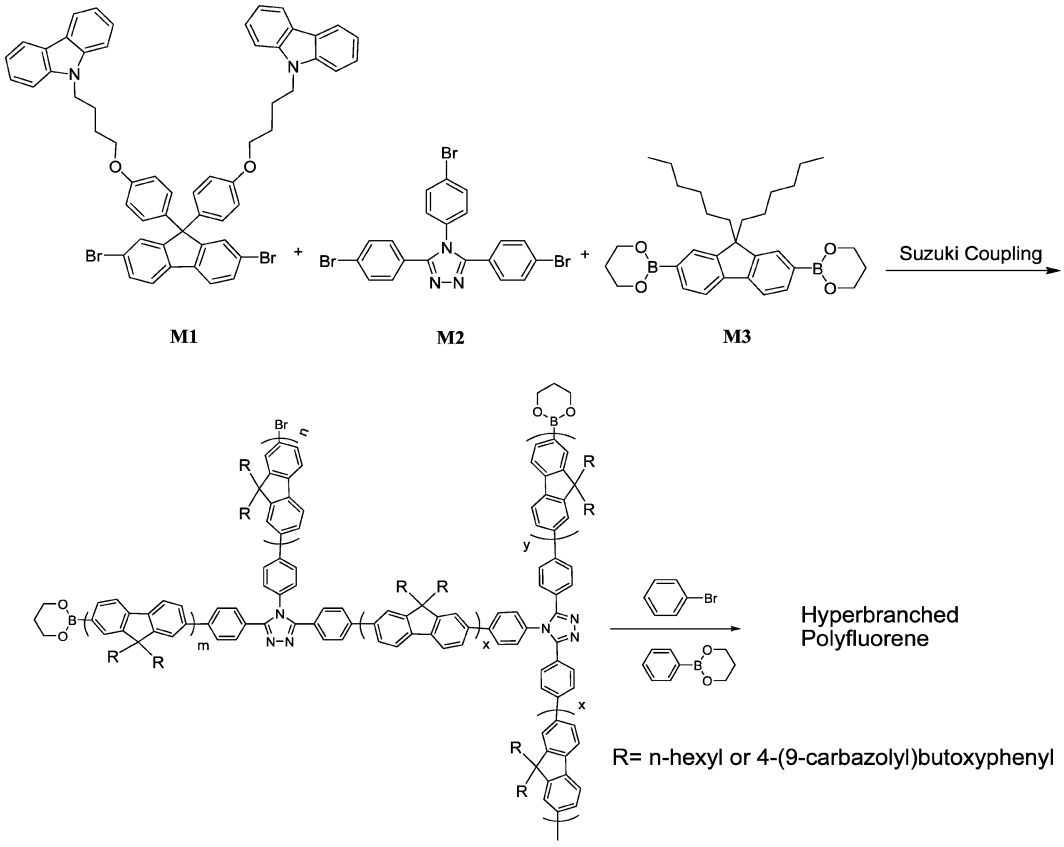


| | M1 | M2 | M3 | $n_{triazole}$ of Feed (mole fraction) |
|---|---|---|---|---|
| **P1** | 1 | 0 | 1 | 0 |
| **PF1** | 10 | 1 | 11.5 | 0.044 |
| **PF2** | 5 | 1 | 6.5 | 0.080 |
| **PF3** | 3 | 1 | 4.5 | 0.118 |
| **PF4** | 2 | 1 | 3.5 | 0.154 |
| **PF5** | 1 | 1 | 2.5 | 0.222 |

solution (4 mL), and ethanol (4 mL) were used. The obtained solid was a deep brown powder (0.145 g, 64%). $^1$H NMR (400 MHz, CDCl3): $\delta$ (ppm) 8.06 (d, $J$ = 7.65 Hz, carbazole rings), 7.78−7.85 (m, Ar−H), 7.63−7.70 (m, Ar−H), 7.55 (m, Ar−H), 7.26−7.48 (m, Ar−H), 6.70 (d, $J$ = 6.44 Hz, Ar−H), 4.30 (t, $J$ = 6.8 Hz, N−$CH_2$), 3.89 (t, $OCH_2$), 2.03−2.17 (m, −$CH_2$−), 1.74 (m, −$CH_2$−), 1.25 (m, −$CH_2$−), 0.93−0.86 (m, −$CH_2$−), 0.70−0.72 (m, −$CH_3$). FT-IR (KBr pellet, cm$^{-1}$): $\nu$ 3045 (Ar−H), 2939, 2922, 2925, 2855, 2360, 1871, 1612, 1597, 1502, 1445, 1414, 1398, 1322, 1246. Anal. Calcd for **P1** ($C_{82}H_{81}N_2O_2$): C, 87.46; H, 7.20; N, 2.49. Found: C, 86.26; H, 7.10; N, 2.58.

## Results and Discussion

**Synthesis and Characterization.** The structure and constitutional composition of the hyperbranched polyfluorenes were estimated from the data of high-resolution NMR spectroscopy and elemental analysis. Linear polymer (**P1**) composed of polyfluorene main chain and carbazole side groups was also prepared for studies of its properties. Figure 1 shows the $^1$H NMR spectrum of **PF1**. The mole ratio of **M1**:**M3** can be readily estimated from the relative areas of the methylene protons of **M1** (a, 1.8 ppm; b, 2.1 ppm) and **M3** (c, 2.0 ppm) residues. The molar ratios of **M1**:**M3** in **PF1**, **PF2**, **PF3**, **PF4** and **PF5** are estimated to be 10:11.8, 5:6.67, 3:4.56, 2:3.51, and 1:2.56, respectively. The attempt to estimate the ratios of the branching triazole and fluorene units was inconclusive due to overlap of their chemical shifts around $\delta$ = 8.0 to 7.2 ppm. However, the ratio of the branching triazole unit (**M2**) can be roughly estimated from the weight percents of carbon and nitrogen obtained in element analysis. The molar ratios (**M1**: **M2**: **M3**) in **PF1**, **PF2**, **PF3**, **PF4**, and **PF5** are estimated to be (10:0.98:11.8), (5:0.80:6.67), (3:0.866:4.38), (2:0.91:3.51), and (1:1:2.56); i.e., the molar fractions of aromatic 1,2,4-triazole residue (**M2**) in **PF1**, **PF2**, **PF3**, **PF4**, and **PF5** are 0.043, 0.064, 0.105, 0.140, and 0.22, respectively. The estimated molar percents are close to the feed ones (22.2−4.4% as shown in Scheme 2) except **PF2** (8.0%). Since the molar ratio of triazole unit in **PF1** is the

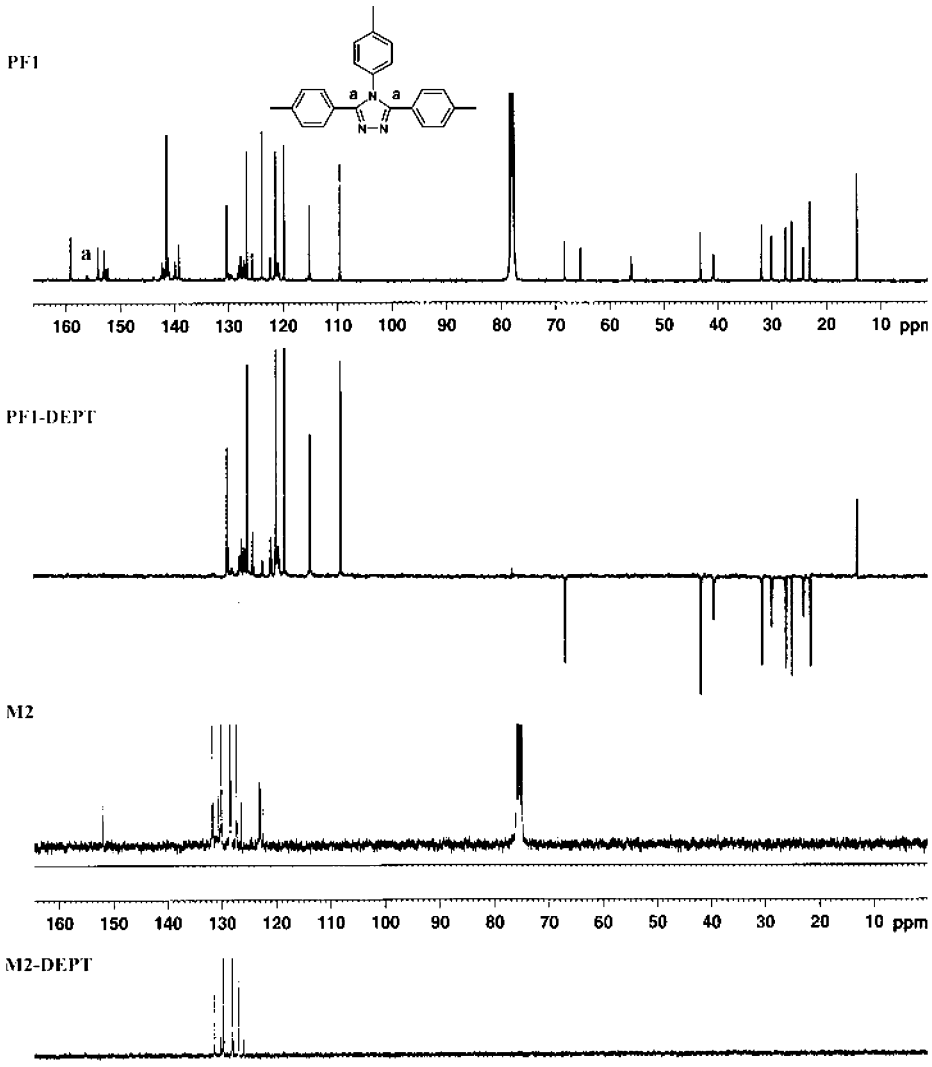


**Figure 2.** $^{13}C$ NMR spectra and DEPT of **PF1** and **M2**.

**Table 1. Polymerization Results of P1 and the Hyperbranched Polymers**

| | reacn time[a] (h) | yield (%) | $M_n$[b] ($\times 10^4$) | $M_w$[b] ($\times 10^4$) | PDI[b] | $T_d$[c] (°C) | $n_{triazole}$[d] (mole fraction) |
|---|---|---|---|---|---|---|---|
| **P1** | 48 | 72 | 1.83 | 2.28 | 1.25 | 420 | 0 |
| **PF1** | 36 | 74 | 0.74 | 1.38 | 1.86 | 446 | 0.043 |
| **PF2** | 20 | 63 | 0.78 | 1.61 | 2.04 | 446 | 0.064 |
| **PF3** | 8 | 72 | 0.97 | 2.49 | 2.57 | 448 | 0.105 |
| **PF4** | 8 | 58 | 0.67 | 2.56 | 3.80 | 456 | 0.140 |
| **PF5** | 6 | 61 | 0.55 | 2.45 | 4.45 | 456 | 0.220 |

[a] The reaction times were chosen to avoid gelation. [b] The temperatures at 5% weight loss. [c] $M_n$, $M_w$, and PDI were determined by gel permeation chromatography using polystyrene standards and $CHCl_3$ as eluent. [d] The molar fractions of the branching triazole unit (**M2**) were estimated from weight percent of carbon and nitrogen obtained in element analysis.

least, therefore, its $^{13}C$ NMR and DEPT135 measurements were adapted to confirm the existence of **M2** residue as shown in Figure 2. The chemical shifts of the C-2,5 of **M2** residue can be observed at 155.8 ppm (a) in $^{13}C$ NMR of **PF1** (100.6 MHz, $CDCl_3$).

As shown in Table 1, the number-average ($M_n$) and weight-average molecular weights ($M_w$) of **PF1**−**PF5**, determined by gel permeation chromatography using mono-disperse polystyrene as calibration standard, are in the range of 5500−9700 and 13800−25600, respectively, with polydispersity indexes (PDI) lying around 1.86−4.45. The copolymers are soluble in common organic solvents such as chloroform, toluene, and 1,1,2,2-tetrachloroethane. Thermal properties of the polymers were evaluated by the TGA under nitrogen atmosphere and their thermal decomposition temperatures ($T_d$) at 5% weight loss are over 446 °C, which are much higher than corresponding linear polymer (**P1**: 420 °C). Neither melting temperature and nor obvious glass-transition temperature was observed below

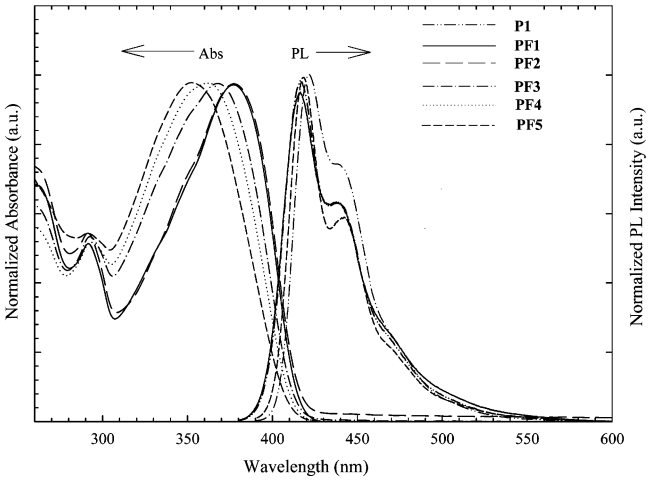


**Figure 3.** Photoluminescence and absorption spectra of **P1** and **PF1**−**PF5** in $CHCl_3$ ($1 \times 10^{-6}$ g/mL). Excitation: 378, 378, 377, 369, 361, and 349 nm for **P1** and **PF1**−**PF5**, respectively.

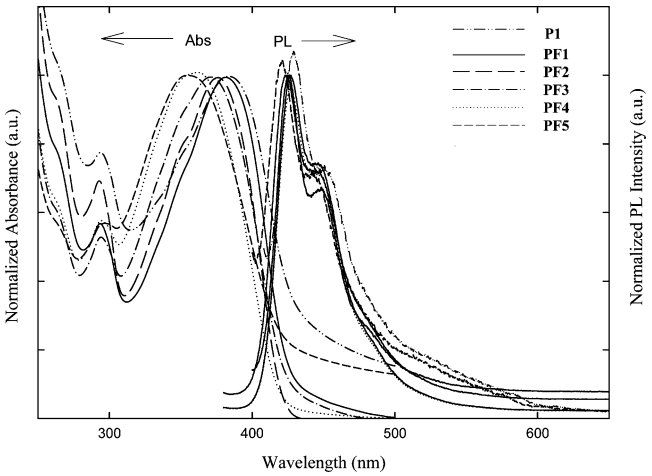


**Figure 4.** Photoluminescence and absorption spectra of **P1** and **PF1**−**PF5** films coated on quartz plate. Excitation: 378, 378, 377, 369, 361, and 349 nm for **P1** and **PF1**−**PF5**, respectively.

**Table 2. Optical Properties of P1 and Hyperbranched Polymers**[b]

| no. | UV−vis $\lambda_{max}$[a] solution (nm) | UV−vis $\lambda_{max}$ film (nm) | PL $\lambda_{max}$[a] solution (nm) | PL $\lambda_{max}$ film (nm) |
|---|---|---|---|---|
| **P1** | 266, 299, 378 | 266, 297, 378 | 421, 440[s] | 427, 449[s] |
| **PF1** | 266, 296, 378 | 266, 297, 378 | 418, 441[s] | 426, 448[s] |
| **PF2** | 266, 296, 377 | 266, 297, 378 | 418, 441[s] | 425, 447[s] |
| **PF3** | 266, 296, 369 | 266, 297, 371 | 417, 440[s] | 425, 447[s] |
| **PF4** | 266, 296, 361 | 266, 297, 362 | 416, 440[s] | 425, 447[s] |
| **PF5** | 266, 296, 349 | 266, 297, 349 | 415, 440[s] | 423, 447[s] |

[a] Concentration: $1 \times 10^{-5}$ M in $CHCl_3$. [b] Superscript s means wavelength of the shoulder.

300 °C on their DSC thermograms, suggesting that they are basically amorphous materials.

**Optical and Photoluminescent Properties.** The optical characteristics of the polymers were investigated both in solution and as cast thin film. Their absorption and photoluminescence (PL) spectra in $CHCl_3$ and in film state are shown in Figure 3 and Figure 4, respectively, and the related spectral maxima are summarized in Table 2. These polymers show absorption maxima around 349−378 nm, both in solution and in the film state, which are attributed to a $\pi-\pi^*$ transition of the conjugated oligofluorene segments. The absorption maximum of **PF1** (378 nm) shows a blue-shift of 29 nm relative to **PF5** (349 nm). Obviously, the conjugation length decreases gradually with increasing branching triazole content (from **PF1** to **PF5**). Moreover, the absorption peaks at 296 and 266 nm can be attributed to the pendent carbazole chromophores. The PL peaks of **P1** and **PF1**−**PF5** in $CHCl_3$ locate around 415−421 nm, which red-shift slightly (ca. 7 nm) relative to those in film state. Previous literature pointed out that although the absorption spectral maxima of oligofluorenes continue to shift to the longer wavelength through $n = 10$ ($n$: number of fluorene units), while their emission maxima remain virtually unchanged beyond $n = 6$.[26] In our system the conjugation length should extend with decreasing molar percent of triazole branch unit in the hyperbranched polymers. For instance, absorption maximum of **PF5** (349 nm) shifts bathochromically to 378 nm of **PF1** and **P1**. The emission spectral maxima, however, remains virtually unchanged, i.e., around 415−421 nm and 423−427 nm in $CHCl_3$ and the film state, respectively. This should be due to efficient excitation energy transfer from short oligofluorenes to longer ones whose fluorene unit number ($n$) is over 6. Interestingly, we found that there exists a linear relationship between $1/\lambda_{max}$ and $1/(1 - n_{triazole})$ as shown in Figure 5, where $\lambda_{max}$ represents the absorption maxima measured in film state

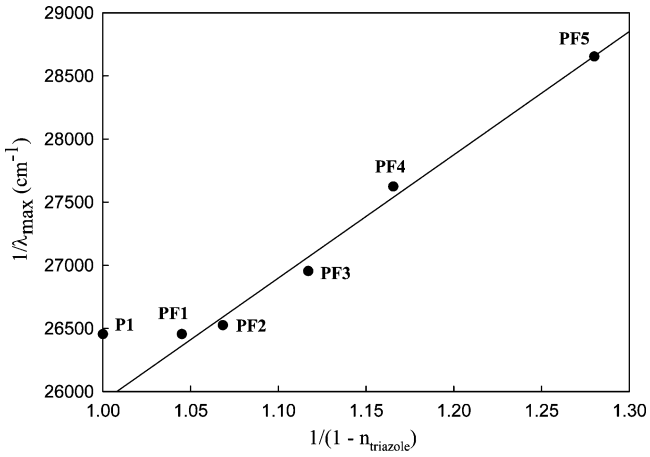


**Figure 5.** Plot of $1/\lambda_{max}$ vs $1/(1 - n_{triazole})$, where $\lambda_{max}$ is the absorption maximum in film state and $n_{triazole}$ is the molar fraction of branching triazole in the hyperbranched polymers.

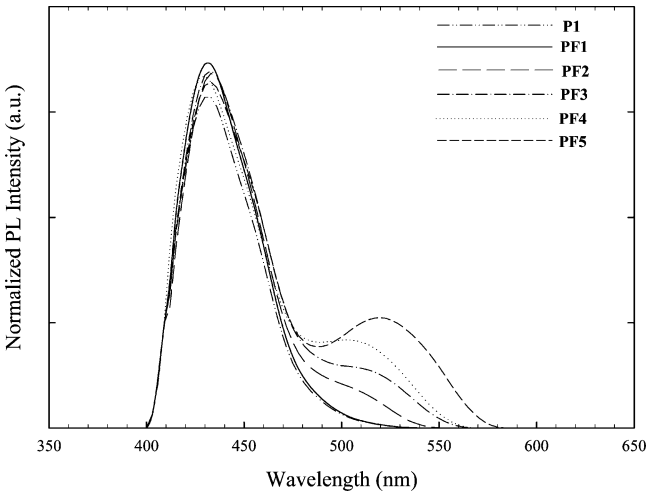


**Figure 6.** PL spectra of **P1** and **PF1**−**PF5** films after annealing at 200 °C in air for 1 h.

and $n_{triazole}$ is the molar fraction of triazole unit calculated from elemental analysis. The linear relationship between $1/\lambda_{max}$ and $1/(1 - n_{triazole})$ indicates that the effective conjugation length of the oligofluorene decreases smoothly with increasing triazole contents.[26] Accordingly, the average conjugation length of a hyperbranched oligofluorene can be estimated from its absorption maximum using the linear plot of $1/\lambda_{max}$ vs $1/(1 - n_{triazole})$.

It is well-known that thermal annealing of polyfluorene usually leads to formation of interchain interaction (excimers) and/or ketonic defects.[7] Figure 6 shows the normalized PL emission spectra of **P1** and **PF1**−**PF5** films after annealing at 200 °C in the air for 2 h. It is noteworthy that no additional band emerges in the PL spectra of **P1** and **PF1** whose triazole molar contents are 0% and 4.3%, respectively. The appearance of additional band is usually undesirable since it changes the pure blue emission to blue-green color.[6] To our best of knowledge no similar stable polyfluorene derivatives annealed in the elevated temperatures in air have been reported. Apparently, with the incorporation of carbarzole pendent groups (**P1**) and/or triazole branching unit (**PF1**), the red-shift and excimer/ketone phenomena of polyfluorene can be reduced significantly. However, normalized PL emission spectra of **PF2**−**PF5** show additional characteristic broad band at about 520 nm after the annealing, and the band intensity enhances gradually with increasing triazole content. Higher degree of branch makes the hyperbranched polymers more three-dimensional to avoid

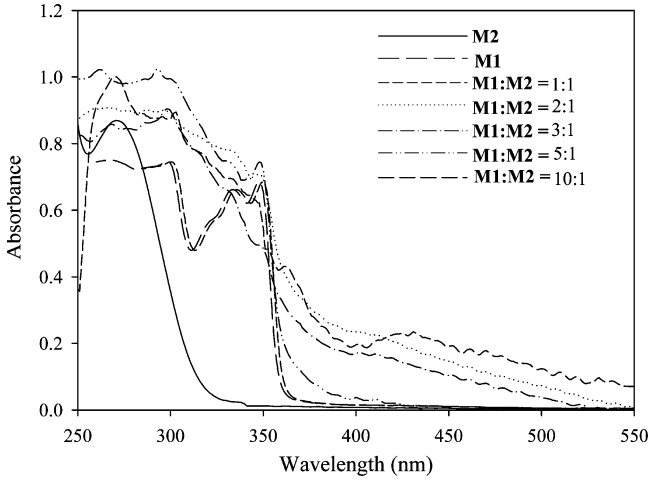


**Figure 7.** Absorption spectra of **M1**, **M2**, and their mixtures (molar ratio of **M1**:**M2** = 1:1, 2:1, 3:1, 5:1 and 10:1) in $CHCl_3$.

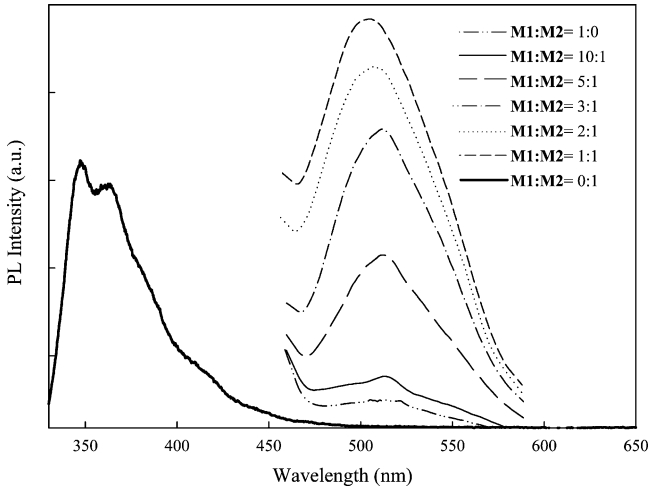


**Figure 8.** PL spectra of mixtures of **M1** and **M2** in $CHCl_3$ ($\lambda_{ex}$ = 440 nm for **M1**:**M2** = 1:0 to 1:1; $\lambda_{ex}$ = 275 nm for **M1**:**M2** = 0:1).

**Table 3. Electrochemical Properties of P1 and Hyperbranched Polymers**

| no. | $E_{onset(ox)}$ (V) vs FOC[a] | $E_{onset(red)}$ (V) vs FOC[a] | $E_{LUMO}$ (eV)[b] | $E_{HOMO}$ (eV)[c] | $E_g^{el}$ (eV)[d] | $E_g^{opt}$ (eV)[e] |
|---|---|---|---|---|---|---|
| **P1** | 0.54 | −2.61 | −2.19 | −5.34 | 3.15 | 2.89 |
| **PF1** | 0.56 | −2.38 | −2.42 | −5.36 | 2.94 | 2.90 |
| **PF2** | 0.59 | −2.36 | −2.44 | −5.39 | 2.95 | 2.93 |
| **PF3** | 0.60 | −2.37 | −2.43 | −5.40 | 2.97 | 2.94 |
| **PF4** | 0.60 | −2.36 | −2.44 | −5.40 | 2.96 | 2.99 |
| **PF5** | 0.61 | −2.36 | −2.44 | −5.41 | 2.97 | 3.00 |

[a] $E_{FOC}$ = 0.48V vs Ag/AgCl. [b] $E_{LUMO} = -(E_{onset(red),FOC} + 4.8)$ eV. [c] $E_{HOMO} = -(E_{onset(ox),FOC} + 4.8)$ eV. [d] $E_g$ = LUMO − HOMO. [e] Band gaps obtained from absorption edge ($E_g = hc/\lambda_{onset}$).

excimer/aggregate formation in addition to bulky carbazole side chain. Therefore, the green emission should not originate from intermolecular interaction. In order to elucidate the origin of this abnormal green emission induced by thermal annealing, we measured the absorption spectra of monomer mixtures (**M1** + **M2**) in $CHCl_3$ (Figure 7). Interestingly, the mixtures with **M1**:**M2** = 1:1, 2:1, 3:1, and 5:1 all exhibited broad absorption band at about 440−450 nm. Moreover, the PL spectra (excitation at 440 nm) of the mixtures with **M1**:**M2** = 1:1, 2:1, 3:1, and 5:1 all exhibited green emission as shown in Figure 8. However, no green emission was observed for **M1**:**M2** = 10:1 and 1:0, which is similar to the result obtained after annealing **PF1** and **P1** at 200 °C for 2 h mentioned above. Therefore, the green emission possibly originates from the complex of triazole and

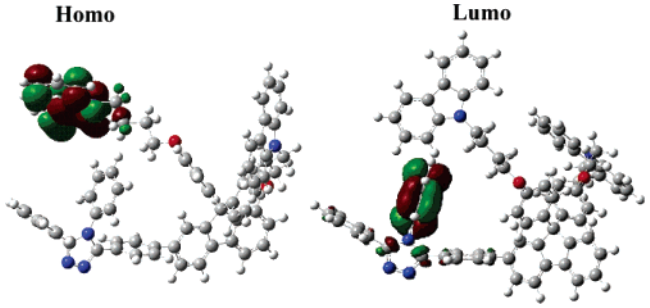


**Figure 9.** Optimized geometries and molecular orbital of linked **M1** and **M2** residues using semiempirical MNDO calculation.

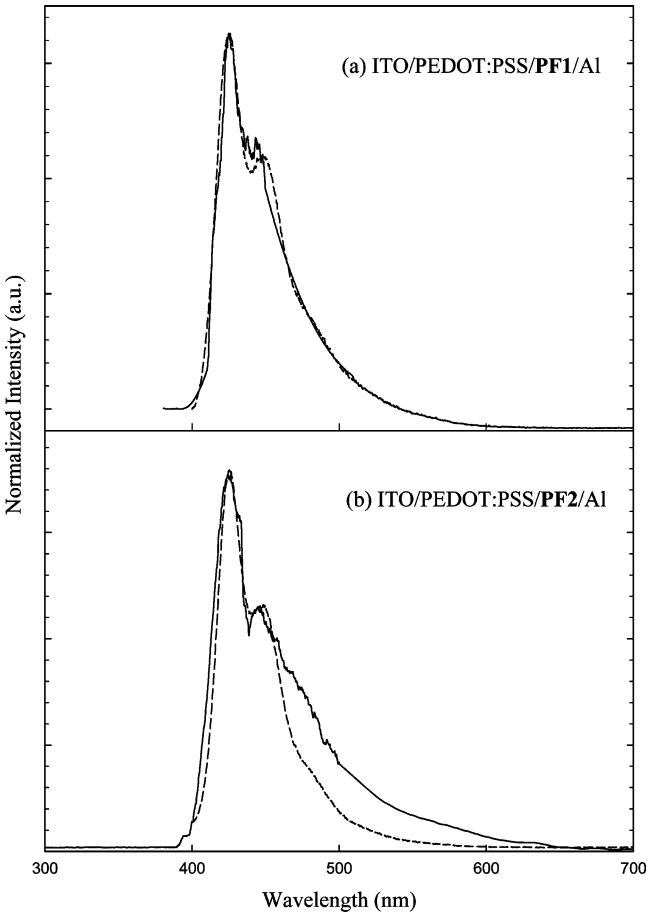


**Figure 10.** Photoluminescent (---) and electroluminescent (−) spectra of **PF1** and **PF2** films.

carbazole units. Accordingly, the green emission becomes more obvious when the molar ratio of **M2** and **M1** is approaching 1. The energy levels of **M1** and **M2** were also estimated from their onset reduction and oxidation potentials measured in acetonitrile. The HOMO and LUMO energy levels of **M1** (**M2**), estimated from the electrochemical data, are −5.41 eV (−6.44 eV) and −1.90 eV (−2.54 eV), respectively. The band gaps between HOMO level of **M1** and LUMO level of **M2** is 2.87 eV, which is corresponding well to the excitation wavelength (440 nm), suggesting that the two monomers form as complex readily.

**Electrochemical Properties.** Cyclic voltammograms of **P1** and **PF1**−**PF5** films coated on a Pt working electrode were measured, and their electrochemical data are summarized in Table 3. For linear polyfluorene **P1**, the onset oxidation (p-doping) and reduction potentials (n-doping) located at +0.54 and −2.61 V, respectively. The onset oxidation potentials of hyperbranched **PF1**−**PF5** shift slightly to 0.56−0.61 V and the onset reduction potentials shift moderately to −2.36 to −2.38

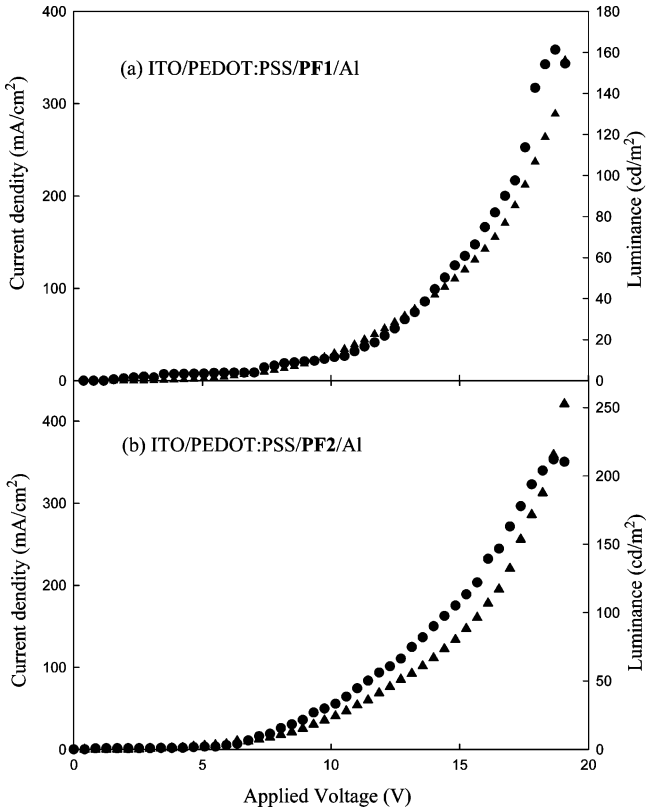


**Figure 11.** Luminance−voltage (●) and current density−voltage (▲) characteristics of the EL devices.

V after incorporating triazole branching units. It is noteworthy that **PF1**−**PF5** possess very similar onset oxidation and reduction potentials. The estimated HOMO and LUMO energy levels of **PF1**−**PF5** are in the range of −5.41 to −5.36 eV and −2.44 to −2.42 eV, respectively, whereas those of **P1** are −5.34 and −2.19 eV. The optimized geometries and molecular orbital (LUMO and HOMO) for linked **M1** and **M2** residues via MNDO semiempirical calculation are depicted in Figure 9,[27] in which the HOMO and LUMO situate at hole- (carbazole) and electron-transporting (triazole) segments, respectively. Accordingly, the oxidation and reduction under a bias will start from carbazole and triazole, respectively. This redox behavior is also expected for **PF1**−**PF5** since they also comprise hole-transporting carbazole pendent groups and electron-transporting triazole segments.

In copoly(aryl ether)s composed of isolated hole- and electron-transporting segments, the oxidation and reduction was proved to start from the former and the latter segments, respectively.[28−30] Recently, this characteristics were also found in linear EL copolymers possess twisted connectors (such as biphenylene) between electron-donor and electro-acceptors segments.[31] In this work, the hyperbranched polymers **PF1**−**PF5** also consist of electron- and hole-transporting segments, and the triazole moiety is connected with fluorene derivatives via a $\sigma$-bond. The twisted structure between them effectively limits delocalization of electronic charges, whose effect is similar to the ether spacer or biphenylene connector mentioned above.[28−31]

**Electroluminescence Properties.** Two-layer EL devices (ITO/PEDOT:PSS/polymer/Al) employing **PF1** and **PF2** as emitting layer were fabricated to investigate their EL spectral charateristics because of their good stability during thermal annealing at 200 °C. The EL spectrum of **PF1** is similar to its PL spectra as shown in Figure 10a. In Figure 10b, the EL of **PF2** reveals a much broader emission in longer wavelength region, which might be due to partial complex formation during device operation. However, no green-blue band emission at 550 nm was observed in EL spectra of **PF1** and **PF2**. This result indicates the hyperbranched polymers could prevent the aggregation or ketonic defects effectively.[7,32] Figure 11 displays the current−voltage ($I-V$) and luminance−voltage ($L-V$) characteristics of the EL devices. The maximum brightness (current efficiency) of **PF1** and **PF2** devices are 161 cd/m$^2$ (0.056 cd/A) and 212 cd/m$^2$ (0.059 cd/A), respectively, which are much higher than that of the **P1** device (48 cd/m$^2$, 0.014 cd/A). This result suggests that incorporation of branching electron-transporting triazole units is effective in improving EL performance of the devices.

## Conclusion

One linear (**P1**) and five hyperbranched polyfluorenes (**PF1**−**PF5**) containing carbazole as pendent and aromatic 1,2,4-triazole as branching units were synthesized and characterized. These hyperbranched polymers can be dissolved in common organic solvents and exhibit good thermal stability ($T_d$ > 420 °C). Their absorption maxima ($\lambda_{max}$) are located at 349−378 nm, and furthermore, a linear relationship between $1/\lambda_{max}$ and $1/(1 - n_{triazole})$ can be correlated. New green emission (~520 nm) appears in the PL spectra of **PF2**−**PF5** after thermal annealing at 200 °C, which have been attributed to complexes formed from carbazole and aromatic 1,2,4-triazole chromophores. The oxidation and reduction start from the carbazole and triazole groups, respectively, due to their isolated characteristics. Two-layer PLED devices (ITO/PEDOT/ **PF1** or **PF2**/Al) have been fabricated and their optical properties investigated, the maximum brightness of **PF1** and **PF2** is 161−212 cd/m$^2$ at about 19 V.

**Acknowledgment.** We thank the National Science Council of the Republic of China for financial aid through Project NSC 95-2221-E006-226-MY3.

## References and Notes

(1) (a) Burroughes, J. H.; Bradley, D. D. C.; Brown, A. R.; Marks, R. N.; Mackay, K.; Friend, R. H.; Bruns, P. L.; Holmes, A. B. *Nature (London)* **1990**, *347*, 539. (b). Blom, P. W. M. *Mater. Sci. Eng.* **2000**, *27*, 53.
(2) Bemius, M. T.; Mike, I.; O'Brien, J.; Wu, W. *Adv. Mater.* **2000**, *12*, 1737.
(3) Kraft, A.; Grimsdale, A. C.; Holmes, A. B. *Angew. Chem., Int. Ed.* **1998**, *37*, 402.
(4) (a) Kreyenschmidt, M.; Klaerner, G.; Fuhrer, T.; Ashenhurst, J.; Karg, S.; Chen, W. D.; Lee, V. Y.; Scoot, J. C.; Miller, R. D. *Macromolecules* **1998**, *31*, 1099. (b) Leclerc, M. *J. Polym. Sci., Part A: Polym. Chem.* **2001**, *39*, 2867. (c) Neher, D. *Macromol. Rapid Commun.* **2001**, *22*, 1365. (e) Becker, S.; Ego, C.; Grimsdale, A. C.; List, E. J. W.; Marsitzky, D.; Pogantsch, A.; Setayesh, S.; Leising, G.; Müllen, K. *Synth. Met.* **2002**, *125*, 73.
(5) Gong, X.; Iyer, P. K.; Moses, D.; Bazan, G. C.; Heeger, A. J.; Xiao, S. S. *Adv. Func. Mater.* **2003**, *13*, 325.
(6) Teetsov, J.; Fox, M. A. *J. Mater. Chem.* **1999**, *9*, 2117.
(7) Zojer, E.; Pogantsch, A.; Hennebicq, E.; Beljonne, D.; Bredas, J. L.; de Freitas, P. S.; Scherf, U. List, E. J. W. *J. Chem. Phys.* **2002**, *117*, 6794.
(8) List, E. J. W.; Guentner, R.; Scandiucci de Freitas, P.; Scherf, U. *Adv. Mater.* **2002**, *14*, 374.
(9) (a) Grell, M.; Knoll, W.; Lupo, D.; Meisel, A.; Miteva, T.; Neher, D.; Nothofer, H. G.; Scherf, U.; Yasuda, A. *Adv. Mater.* **1999**, *11*, 671. (b) List, E. J. W.; Partee, J.; Shinar, J.; Scherf, U.; Müllen, K.; Graupner, W.; Petritsch, K.; Zojer, E.; Leising, G. *Phys. Rev. B* **2000**, *61*, 10807.
(10) (a) Pschirer, N. G.; Bunz, U. H. F. *Macromolecules* **2000**, *33*, 3961. (b) Schmitt, C.; Nothofer, H. G.; Falcou, A.; Scherf, U. *Macromol. Rapid Commun.* **2001**, *22*, 624. (c) Kreyenschmidt. M.; Klärner, Fuhrer, T.; Ashenhurst, J.; Karg, S.; Chen, W. D.; Lee, V. Y.; Scott, J. C.; Miller, R. D. *Macromolecules* **1998**, *31*, 1099. (d) Lee, J. I. G.; Daver, M. H.; Miller, R. D. *Synth. Met.* **1999**, *102*, 1087. (e) Xia, C.;

Advincula, R. C. *Macromolecules* **2001**, *34*, 5854. (f) Liu, B.; Yu. W. L.; Lai, Y. H.; Huang, W. *Macromolecules* **2000**, *33*, 8945.
(11) (a) Setayesh, S.; Grimsdale, A. C.; Weil, T.; Enkelmann, V.; Müllen, K.; Meghdadi, F.; List, E. J. W.; Leising, G. *J. Am. Chem. Soc.* **2001**, *123*, 946. (b) Marsitzky, D.; Vestberg, R.; Blainey, P.; Tang, B. T.; Hawker, C. J.; Carter, K. R. *J. Am. Chem. Soc.* **2001**, *123*, 6965. (c) Klärner, G.; Miller, R. D.; Hawker, C. J. *Polym. Prepr.* **1998**, *39*, 1006. (d) Berresheim, A. J.; Müller, M. Müllen, K. *Chem. Rev.* **1999**, *99*, 1747. (e) Morgenroth, F.; Reuter, E.; Müllen, K. *Angew. Chem.* **1997**, *109*, 647; *Angew. Chem., Int. Ed. Engl.* **1997**, *36*, 631.
(12) (a) Klärner, G.; Miller, R. D.; Hawker, C. J. *Polymer. Prepr.* **1998**, 1047. (b) Miteva, T.; Meisel, A.; Knoll, W.; Nothofer, H. G.; Scherf, U.; Müller, D. C.; Meerholz, K.; Yasuda, A.; Neher, D. *Adv. Mater.* **2001**, *13*, 565. (c) Lee, J. L.; Hwang, D. *Synth. Met.* **2000**, *111*, 195.
(13) (a) Klaerner, G.; Lee, J. L.; Lee, V. Y.; Chan, E.; Chen, J. P.; Nelson, A.; Markiewicz, D.; Siemens, R.; Scott, J. C.; Miller, R. D. *Chem. Mater.* **1999**, *11*, 1800. (b) Chen. J. P.; Klaerner, G.; Lee, J. I.; Markiewicz, D.; Lee, V. Y.; Miller, R. D.; Scott, J. C. *Synth. Met.* **1999**, *107*, 129. (c) Cho, H. J.; Jung, B. J.; Cho, N. S.; Lee, J.; Shim, H. K. *Macromolecules* **2003**, *36*, 6704.
(14) (a) Müllen, K.; Wegner, G., Eds. *Electronic Materials: The Oligomer Approach*; Wiley-VCH: Weinheim, Germany, 1998. (b) Geng, Y.; Trajkovska, A.; Katsis, D.; Ou, J. J.; Culligan, S. W.; Chen, S. H. *J. Am. Chem. Soc.* **2002**, *124*, 8337. (c) Porzio, W.; Botta, C.; Destri, S.; Pasini, M. *Synth. Met.* **2001**, *122*, 7. (d) Lee, S. H.; Tsutsui, T. *Thin Solid Films* **2000**, *363*, 76. (e) Jo, J.; Höger, S.; Wegner, G.; Yoon, D. Y. *Polym. Prepr.* **2002**, *43*, 1118.
(15) Shirota, Y.; Kuwabara, Y.; Inada, H.; Wakimoto, T.; Nakada, H.; Yonamoto, Y.; Kawai, S.; Imai, K. *Appl. Phys. Lett.* **1994**, *65*, 807.
(16) Bettenhausen, J.; Greczmiel, M.; Jandke, M.; Strohriegl, P. *Synth. Met.* **1997**, *97*, 223.
(17) Halim, M.; Samuel, I. D. W.; Pillow, J. N. G.; Bourn, P. L. *Synth. Met.* **1999**, *102*, 1113.
(18) Scott, M. G.; Fréchet, J. M. J. *Chem. Rev.* **2001**, *101*, 3819.
(19) Robinson, M. R.; Wang, S.; Bazan, G. C.; Cao, Y. *Adv. Mater.* **2000**, *12*, 1701.
(20) Fréchet, J. M. J. *Science* **1994**, *263*, 1710.
(21) Li, J.; Bo, Z. *Macromolecules* **2004**, *37*, 2013.
(22) Xin, Y.; Wen, G.-A.; Zeng, W.-J.; Zhao, L.; Zhu, X.-R.; Fan, Q.-L.; Feng, J.-C.; Wang, L.-H.; Wei, W.; Peng, B.; Cao, Y.; Huang, W. *Macromolecules* **2005**, *38*, 6755.
(23) Ranger, M.; Leclerc, M. *Macromolecules* **1999**, *32*, 3306.
(24) Bo, Z.; Zhang, W.; Zhang, X.; Zhang, C.; Shen, J. *Macromol. Chem. Phys.***1998**, *199*, 1323.
(25) Liu, Y.; Liu, M. S.; Jen, A. K. Y. *Acta Polym.* **1999**, *50*, 105.
(26) Klaerner, G.; Miller, R. D. *Macromolecules* **1998**, *31*, 2007.
(27) MNDO semi-empirical calculations and molecular orbitals were performed with Gaussian R 98W and Gauss View 3.09 by Gaussian, Inc.
(28) Hwang, S.-W.; Chen, Y. *Macromolecules* **2002**, *35*, 5438.
(29) Hwang, S.-W.; Chen, Y.; Chen, S.-H. *J. Polym. Sci., Part B: Polym Phys.* **2004**, *42*, 333.
(30) Chen, S.-H.; Hwang, S.-W.; Chen, Y. *J. Polym. Sci., Part A: Polym. Chem.* **2004**, *42*, 883.
(31) (a) Chen, S.-H.; Chen, Y. *Macromolecules* **2005**, *38*, 53. (b) Chen, S.-H.; Chen, Y. *J. Polym. Sci.; Part A: Polym. Chem.* **2006**, *44*, 4514. (c) Chen, S.-H.; Chen, Y. *Macromol. Chem. Phys.* **2006**, *207*, 1070.
(32) Weinfertner, K.-H.; Fujikawa, H.; Tokito, S.; Taga, Y. *Appl. Phys. Lett.* **2000**, *76*, 2502.

MA070045L